

On the scaling in the rotational dynamics of molecular probes in salol and ortho-terphenyl: a possible role of the energy landscape basins

This article has been downloaded from IOPscience. Please scroll down to see the full text article.

2006 J. Phys.: Condens. Matter 18 931

(<http://iopscience.iop.org/0953-8984/18/3/011>)

View [the table of contents for this issue](#), or go to the [journal homepage](#) for more

Download details:

IP Address: 129.252.86.83

The article was downloaded on 28/05/2010 at 08:49

Please note that [terms and conditions apply](#).

# On the scaling in the rotational dynamics of molecular probes in salol and ortho-terphenyl: a possible role of the energy landscape basins

L Andreozzi<sup>1</sup>, M Faetti and M Giordano

Dipartimento di Fisica, Università di Pisa, Largo Pontecorvo 3, Pisa I-56127, Italy  
and  
CNR, INFM, PolyLab, Largo Pontecorvo 3, Pisa-56127, Italy

E-mail: [laura.andreozzi@df.unipi.it](mailto:laura.andreozzi@df.unipi.it)

Received 5 July 2005, in final form 16 November 2005

Published 6 January 2006

Online at [stacks.iop.org/JPhysCM/18/931](http://stacks.iop.org/JPhysCM/18/931)

## Abstract

The reorientational dynamics of a stiff paramagnetic tracer dissolved in the glass former salol is investigated by means of electron spin resonance over a broad temperature range. The Debye–Stokes–Einstein law describing rotational diffusion in simple liquids is found to break down in the supercooled region where the diffusion is less temperature dependent than the viscosity. Over a large temperature interval a simple power law relates diffusion and viscosity, whereas at lower temperatures the decoupling is stronger and an activated dynamics is observed. These experiments are discussed together with previous data concerning other tracer/glass former couples. Starting from some observed common features, an attempt is made to obtain a unifying interpretation of the data in the framework of the energy landscape picture.

## 1. Introduction

Microscopic and macroscopic transport properties of liquids are related by the Stokes–Einstein (SE) and Debye–Stokes–Einstein (DSE) laws, concerning translational and rotational dynamics respectively [1]. These relations state that the diffusion coefficients depend linearly on the ratio  $T/\eta$ ,  $\eta$  being the shear viscosity of the fluid. The derivation of both SE and DSE laws rests on classical hydrodynamics [2] and on the Langevin formulation of Brownian motion [3], where the liquid is treated as continuous, homogeneous and instantaneously reacting, and the diffusing body is assumed larger than the molecules of the fluid.

In spite of the above assumptions, SE and DSE usually work very well down to the molecular length scale in normal fluids, with viscosity lower than about  $10^{-1}$  Pa s [1]. On the other hand, deviations could be expected in supercooled liquids and polymers where a

<sup>1</sup> Author to whom any correspondence should be addressed.

dramatic increasing of viscosity is observed on approaching the glass transition. Indeed, several experimental works evidenced a breakdown of the SE relation [4–9], with a decoupling of translational diffusion and viscosity. However, the decoupling is only partial in character. In fact it has been recognized that in supercooled liquids the usual SE law seems to be systematically replaced by a fractional scaling law [10]:

$$D_t \propto \left(\frac{\eta}{T}\right)^{-\xi}. \quad (1)$$

Equation (1) is usually referred to as the fractional Stokes–Einstein (FSE) law. The value of the coupling exponent  $0 < \xi < 1$  depends on both the diffusing particle and the specific fluid.

Several theoretical approaches [11–13] suggested that the decoupling between microscopic transport and viscosity was a signature of heterogeneous dynamics in the deeply supercooled regime, whereas other explanations are based on a frustrated lattice gas model [14] or energy landscape approaches [15, 16].

As far as the rotational diffusion is concerned, the state of the art seems to be less conclusive. Several different experimental works in the last few years found that the DSE law underestimates the rotational diffusion of tracers in supercooled liquids and polymers [7, 17–21], but in other studies only small deviations from the DSE law were observed even close to  $T_g$  [6, 22–24]. This scenario suggests that very important roles in the dynamical results of rotation experiments are played by the length scale probed by the tracer and the timescale selected by the experimental technique. In this respect, electron spin resonance spectroscopy (ESR) deserves consideration due to its well known sensitivity [21, 25–29] to the scales of time and length which should mark the crossover from *liquid-like* to *solid-like* behaviour in glass forming liquids [30]. Indeed, by means of linear and non-linear ESR studies of the reorientation mechanism of different molecular probes dissolved in low molecular weight glass formers [18, 20, 31] and polymers [19, 32, 33], the possibility of a fractional coupling between diffusion and viscosity has been demonstrated also for rotational dynamics (the FDSE law). A similar behaviour was also evidenced from non-radiative decay time measurements [17] on molecular glass formers and from fluorescence experiments on polymers [7]. The temperature ranges where the FDSE law holds and the values of the coupling exponent were found to depend on the diffusing molecule/host matrix couple, so that a unifying interpretation of the experiments is quite complex.

In this paper, additional ESR experimental data concerning the rotational diffusion of the stiff paramagnetic tracer Cholestane dissolved in the glass former salol are presented and analysed together with previous results concerning the rotational dynamics of a different tracer in the same material [31], and the same tracers in a different material [18].

## 2. Experimental details

### 2.1. ESR spectroscopy: an overview

Among the different experimental techniques which can be used to investigate the rotational dynamics in simple and supercooled liquids, ESR spectroscopy plays an important role due to its high sensitivity to the details of the reorientational processes [25, 27–29, 34, 35]. Suitable paramagnetic molecular tracers are usually dissolved in low concentration in the selected material because glass forming systems are usually diamagnetic in character.

In an ESR experiment the spin system is coupled to the molecular probe rotation via the anisotropy of the Zeeman and hyperfine magnetic interactions [35, 36] which, fluctuating at the microscopic times of the lattice, relaxes the magnetization and broadens the lineshape.

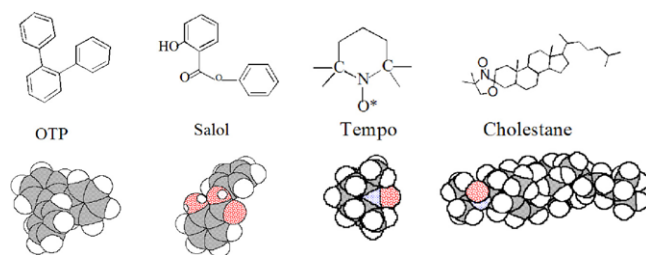


**Figure 1.** Chemical structures and 3D models of the glass formers and the probes used in this work.

(This figure is in colour only in the electronic version)

**Table 1.** Characteristic temperatures of OTP and salol.

	$T_m$ (K)	$T_c$ (K)	$T_g$ (K)
Salol	315	260	220
OTP	331	290	243

The properties of the environmental dynamics are extracted by evaluating the lineshape with suitable numerical algorithms [35, 37]. A stochastic description is assumed for the rotational dynamics. Wigner rotation matrices of rank  $l$  [38] provide a suitable basis for expanding the conditional probability of the stochastic process. Unlike other spectroscopies which are sensitive to the fluctuations of Wigner matrices with  $l = 1$  (dielectric spectroscopy, infrared spectroscopy) or  $l = 2$  (Raman, depolarization of fluorescence, Kerr effect), ESR spectroscopy in the slow motion regime [37] is sensitive to Wigner matrices of even rank [25, 37]. This feature determines the fine details of the ESR lineshape allowing the convenient evaluation of the presence of different rotation mechanisms [25, 34, 39].

## 2.2. Experimental procedures

We consider here ESR studies of the spin probes Tempo (2,2,6,6 tetramethyl-piperidin-1-oxyl, 98% Aldrich) and Cholestane (4',4'-dimethyl-spiro(5 $\alpha$ -cholestane-3,2'-oxazolidin)-3'-yloxy, Aldrich) dissolved in OTP (ortho-terphenyl, 99% Aldrich) and in salol (phenyl salicylate, 99% Aldrich). Salol and OTP are currently considered as model molecular glass formers and widely characterized in the literature. Chemical structures and 3D models of the glass formers and probes are shown in figure 1.

Both the tracers are well characterized as stiff radicals belonging to the nitroxide spin probes [40]. Their different geometries and sizes should be noted. The Tempo tracer is almost spherical, with its van der Waals radius comparable with those of the OTP and salol molecules,  $r_{\text{Tempo}} \sim 0.34$  nm,  $r_{\text{OTP}} \sim 0.37$  nm,  $r_{\text{salol}} \sim 0.34$  nm. In contrast, the Cholestane spin probe can be sketched as a prolate ellipsoid (rod-like) with semi-axes of about 1 and 0.3 nm respectively.

The melting ( $T_m$ ), critical ( $T_c$ ) and glass transition ( $T_g$ ) temperatures for salol and OTP are reported in table 1 [41–49].  $T_c$  is the critical temperature predicted by the mode coupling theory [50].  $T_g$  and  $T_m$  literature temperatures were verified with differential scanning calorimetry experiments carried out at 10 K min<sup>-1</sup>.

The samples were prepared by dissolving the radical in the selected glass former, at a concentration of 10<sup>-3</sup> mol l<sup>-1</sup>. The samples were sealed in standard quartz tubes for the

ESR experiments, after degassing with ultrapure nitrogen for times longer than 1 h at a temperature slightly above the melting point. The above probe concentration had no detectable plasticization effects on the glass former, as verified by differential scanning calorimetry measurements. After more dilution of the guest in the host matrix, no change was shown by the ESR lineshape, which in the low concentration regime is solely determined by the rotational dynamics of the probe molecule. ESR measurements were carried out, by using a Bruker ER200D spectrometer equipped with an X band bridge and an NMR gaussmeter ER035M. Temperature was controlled with a gas flow, variable temperature unit with stability of 0.1 K and experiments were performed over broad temperature ranges including the main characteristic temperatures of the glass formers.

After quenching from above the melting temperature, ESR lineshapes were recorded on heating after ageing the sample for about 20 min at the temperatures selected for the measurement. The signal/noise ratio was quite good ( $10^4$ ), so the errors on the rotational correlation times are mainly due to the numerical simulations of the ESR spectra ( $\sim 5\%$ ). The values of the magnetic parameters of the probe molecules dissolved in salol and OTP were obtained by careful analyses of the experimental powder lineshapes according to a procedure detailed elsewhere [51].

### 3. Results

Due to its almost cylindrical shape, the rotational diffusion of the Cholestane spin probe is usually well described in terms of an anisotropic diffusional mechanism [18], which introduces a spinning diffusion coefficient  $D_{\parallel}$  for the reorientation around the long axis and a tumbling diffusion constant  $D_{\perp}$  for the rotations of the long axis itself. This is also true for the rotation of Cholestane in salol, as shown in figure 2 where some representative experimental ESR spectra are reported together with the pertinent theoretical simulations. The agreement is apparent. One can also appreciate the strong temperature dependence of the ESR lineshape, confirming the high sensitivity of the technique to the dynamics. Further details on the ESR lineshape analysis, and also for the other guest/host system considered in this work, can be found in [18, 25, 31, 34].

In figure 3 the temperature dependence of the diffusion coefficients for the Cholestane tracer in salol is shown for the whole investigation temperature range. By inspection, for both the spinning and the tumbling motions, three different dynamical regimes are easily identified. In the highest temperature regions the diffusion process is well described by the classical hydrodynamics and the DSE scaling holds. Indeed, the continuous lines in figure 3 are the inverse of the literature viscosity data [42–44] over the temperature scaled by proper constants. On lowering the temperature, a breakdown of the DSE law is observed at a characteristic temperature  $T_0$  (298 and 292 K for the spinning and tumbling reorientations respectively). Below such temperatures, rotational diffusion and viscosity partially decouple, with the reorientation exhibiting enhanced diffusion. In this intermediate dynamical region the temperature dependence of the rotational diffusion is well accounted for by a fractional Debye–Stokes–Einstein law (the FDSE law):

$$D_{\parallel,\perp} = C_{\parallel,\perp} \left( \frac{\eta}{T} \right)^{-\xi_{\parallel,\perp}}. \quad (2)$$

The dotted lines of figure 3 represent the best fits of the experimental data with equation (2). As regards the fractional coupling parameters, we found  $\xi = 0.7 \pm 0.06$  and  $\xi = 0.67 \pm 0.06$  for the spinning and tumbling rotations respectively. It should be emphasized that the intermediate regions extend for about 40 K with a variation in the diffusion coefficients of more than two orders of magnitude.

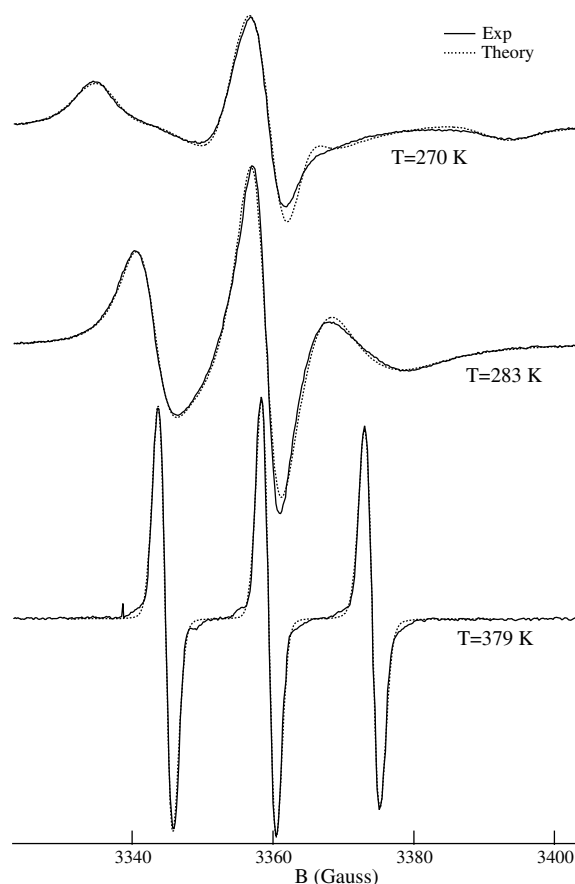


**Figure 2.** Experimental ESR lineshapes of Cholestane in salol recorded at different temperatures. The dotted lines are the theoretical predictions obtained by assuming in the simulation algorithm an anisotropic diffusion mechanism.

Finally, at lower temperatures below  $T_B$ , a greater decoupling between reorientation and viscosity is observed and the activated behaviour signals that diffusion takes place in a solid-like environment.

These results were not unexpected because very similar behaviours were observed in various glass forming systems by using other spectroscopies [52] and with ESR for the same tracer dissolved in OTP [18]. Furthermore, the presence of the same dynamical regions was evidenced also for the molecular spin probe Tempo dissolved in both OTP [18] and salol [31]. In figure 4 the experimental data concerning the reorientations of both the tracers in OTP are collected, whereas figure 5 shows the case for salol. Note that the reorientation mechanism for the Tempo tracer, due to its almost spherical shape, is characterized by only one diffusion coefficient.

Looking at these two figures, the existence of a common general scenario consisting of an high temperature liquid-like region, an intermediate FDSE regime and a low temperature solid-like behaviour is apparent. This is the first remarkable result of our studies. In fact for all the tracer/glass former couples investigated we evidenced the presence of a breakdown of classical hydrodynamics and the existence of regimes of fractional coupling between rotational diffusion and viscosity.

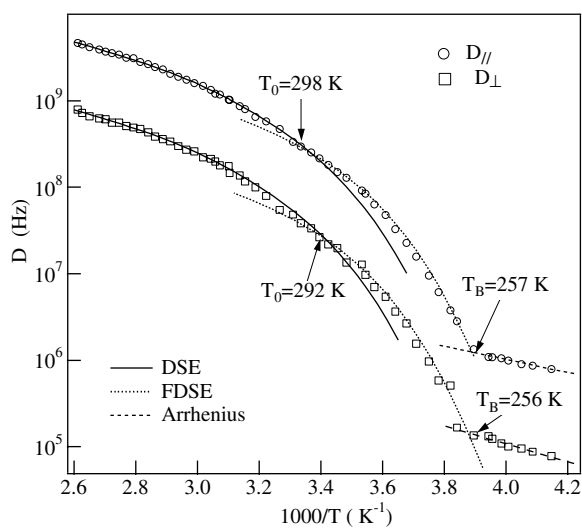


**Figure 3.** Temperature dependence of the spinning and tumbling diffusion coefficients of Cholestane dissolved in salol.  $T_0$  and  $T_B$  are the temperatures where the FDSE law sets in and breaks down respectively.

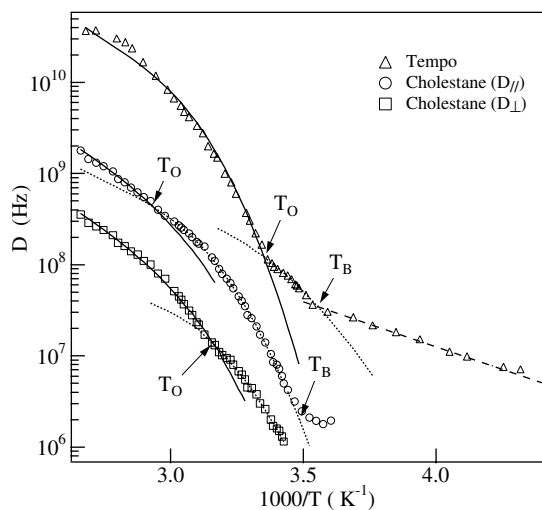


**Figure 4.** Temperature dependence of the diffusion coefficients of Tempo and Cholestane spin probes in OTP.

#### 4. Discussion

The question arises of a coherent interpretation of this phenomenology. In fact a more quantitative analysis shows that the breakdown temperatures and the coupling parameters of the FDSE law,  $\xi$ , depend on both the specific molecular tracer and the selected glass forming liquid as can be observed by inspecting table 2.

If one looks only at the behaviour of the Cholestane probe, it could be argued that the breakdown of the DSE scaling has to be related to some growing relaxation timescale of

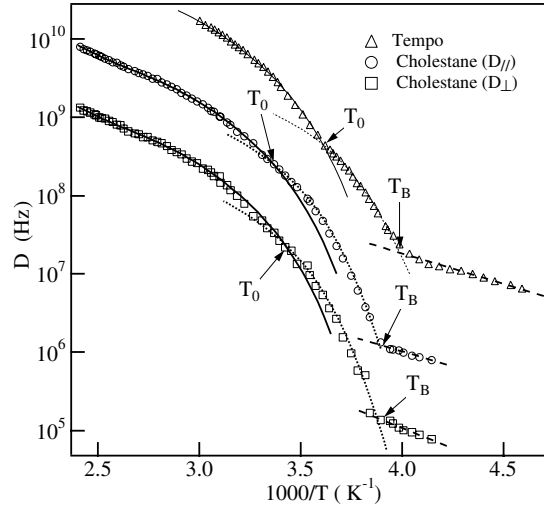


**Figure 5.** Diffusion coefficients of Tempo and Cholestane dissolved in salol.

**Table 2.** Main physical parameters for the rotational diffusion of Tempo and Cholestane tracers dissolved in OTP and salol.  $T_0$  and  $T_B$  are the onset and breakdown temperatures of the FDSE law and  $\Delta T$  is their difference.

	$T_0$ (K)	$T_B$ (K)	$\Delta T$ (K)	$\xi$
Tempo/salol $D$	278	251	27	$0.46 \pm 0.04$
Cholestane/salol $D_{\parallel}$	298	257	41	$0.70 \pm 0.06$
Cholestane/salol $D_{\perp}$	292	256	36	$0.67 \pm 0.06$
Tempo/OTP $D$	298	280	18	$0.28 \pm 0.04$
Cholestane/OTP $D_{\parallel}$	340	288	52	$0.73 \pm 0.06$
Cholestane/OTP $D_{\perp}$	316	—	—	$0.58 \pm 0.06$

the host. In fact, in both the glass formers, the decoupling between spinning rotation and structural relaxation takes place at a temperature higher than that of the tumbling motion, the latter being related to a higher steric hindrance and consequently characterized by a slower dynamics. Furthermore, the breakdown takes place at very similar values of the viscosity of the two liquids: for the spinning rotation  $\eta(T_B^{\text{OTP}}) \approx 0.14$  P and  $\eta(T_B^{\text{salol}}) \approx 0.20$  P. This interpretation, however, seems to be ruled out by the behaviour of the Tempo tracer which is smaller than Cholestane probe and therefore exhibits faster dynamics, but in both the glass formers it follows the DSE scaling down to lower temperatures. These findings show that other relevant parameters have to be taken into account in order to explain the observed phenomenology. In this respect, several works [11–13] suggested that a fundamental role could be played by the presence of dynamical heterogeneities, which is a salient feature of supercooled fluids [13]. As far as the rotational diffusion is concerned, a phenomenological approach [18] introduced dynamic heterogeneity and the cooperativity by modifying the ordinary diffusion model, and provided an analytical expression for the coupling parameter  $\xi$ . The values  $\xi = 0.25$  and  $0.5$  were obtained for a spherical rotating stiff particle when the reorientation of the tracer needs the collective motion of  $m = 2$  and  $4$  host molecules. These values are in agreement with the results obtained for the Tempo probe dissolved in OTP and salol respectively. However the model fails to predict the experimental exponent for geometries other than spherical.



**Table 3.** Crossover temperatures of the rotational diffusion of Tempo and Cholestane dissolved in OTP and salol expressed in the temperature scale of the LJM [53].

	$T_0^*$	$T_B^*$	$\Delta T^*$
Tempo/salol $D$	0.465	0.420	0.045
Cholestane/salol $D_{\parallel}$	0.5	0.430	0.069
Cholestane/salol $D_{\perp}$	0.489	0.428	0.060
Tempo/OTP $D$	0.447	0.420	0.027
Cholestane/OTP $D_{\parallel}$	0.510	0.432	0.078
Cholestane/OTP $D_{\perp}$	0.474	—	—

The above discussion shows that a comprehensive and conclusive interpretation of the observed breakdown of both SE and DSE scalings, and the consequent onset of the fractional regimes, is still lacking. However the experimental data reported in table 2 contain an important regularity. It should be noted in fact that the smaller the coupling parameter value, the smaller the temperature range where the FDSE scaling holds.

This finding is formalized by recognizing that the following relationship is verified within the experimental errors for OTP and salol for both the Tempo and Cholestane rotations:

$$\frac{\Delta T}{\xi \cdot T_c} = \text{const.} \quad (3)$$

Even if empirical in character, and not yet understood in the framework of any theoretical model, equation (3) deserves consideration due to its possible predictive power.

Before concluding this work, we attempt to discuss our data in terms of a numerical study [53] based on the energy landscape paradigm [30, 54]. The landscape  $3N$ -dimensional hypersurface is defined by the potential energy of the system and shows a complicated topology with local minima and energy barriers. At a given temperature, the properties of the system are provided by the sampled basins of the landscape and by their accessibility. In [53], it was suggested that diffusion in liquids is a process dominated by thermodynamics and the average energy of the inherent structures was studied as a marker of dynamics in a model system, the widely used 80–20 Lennard-Jones binary mixture (LJM) [55]. Temperature regions and crossovers were identified and connected to the onset of slow and activated dynamics. In particular, evident changes in the local topography of the sampled landscape were found in the temperature range  $0.45 < T < 0.5$  ( $T_c = 0.435$ ) whereas the onset of activated dynamics was collocated at  $T = 0.425$ . Here the temperatures are reported on the molecular dynamics reduced scale where the critical temperature of mode coupling theory is 0.435. The attempt at connecting our data with Sastry's findings is validated by the works by Takahara *et al* [56], reporting the small value of the thermal expansivity of OTP, by Ferrer *et al* [57], proving that the dominant thermodynamic variable is temperature for fragile glass formers at 1 atm, and by Schug *et al* [58], finding that the fragility of salol and OTP exhibits no appreciable variations at pressures near to the ambient ones. In order to compare our results with the findings of [53] we report our data on the rotational diffusion on the reduced temperature scale simply defined by  $T^* = T \cdot (0.435/T_c)$ . Such values are collected in table 3.

By inspection, a connection between the rotational dynamics features and the topography of the energy landscape described in [53] can be suggested. In fact, interestingly enough, the  $T_B^*$  values, signalling the crossover to activated regimes, range from 0.420 to 0.432, in agreement with the temperature  $T = 0.425$  at which activated dynamics takes place in the LJM model [53].

The  $T_B^*$  values detected via ESR are slightly greater and smaller than 0.425, and characterize the dynamics respectively of Cholestane and Tempo probes dissolved in both OTP

and salol. These slight differences (amounting to few degrees on the absolute  $T$  scale) could be ascribed to different structural properties such as flexibility or size of the glass former with respect to the tracer. Thus one is inclined to conclude that deeper basins are 'felt' by the Tempo molecular tracer. On the other hand, the greater  $T_B^*$  values provided by the rotation of Cholestane are very close to the critical temperature  $T_c^*$ . It appears therefore that the length scale probed by the guest molecule plays an important role in determining the temperatures at which crossover to activated dynamics is observed. This is in agreement with the statement of the landscape paradigm that 'for every potential of interaction there is an energy of the order of  $RT_B$  below which there are no states other than vibrational states' [59]. At higher temperatures, the onset of fractional laws in our experiments of rotational dynamics arises at temperatures ranging in the interval 0.447–0.51. This is the range of temperatures where, according to figure 4 of [53], the landscape dominated regime sets in in the host system that is able to explore different basins even with very low excitation energy. The lower and upper limits correspond to Tempo and Cholestane probes in OTP, suggesting the importance of the molecular size for picturing the details of the excitation profile of the host landscape.

## 5. Conclusions

The rotational dynamics of a molecular probe dissolved in the glass former salol has been studied by means of ESR experiments. A breakdown of classical hydrodynamics was observed in the supercooled region, where rotational diffusion and viscosity were related by a power law (the FDSE law). At lower temperatures the activated dynamics evidenced an even greater decoupling between tracer reorientation and structural relaxation. These results support our previous findings concerning different tracer/glass former couples, and confirm the existence of fractional couplings between diffusion and viscosity for the rotational dynamics also.

Moreover the data on rotational dynamics of different tracers in salol and OTP have been considered with reference to the literature studies of molecular dynamics on a model system, where the dynamics of glass formers was related to the features of the potential energy hypersurface explored by the liquid at different temperatures. There appears to be a possibility of a correspondence between the signatures observed in the tracer dynamics and those signalling the onset of both the landscape dominated regime and the activated dynamics in the energy landscape profile of fragile glass formers.

## References

- [1] Egelstaff P A 1994 *An Introduction to the Liquid State* (Oxford: Clarendon)
- [2] Lamb H 1993 *Hydrodynamics* (Cambridge: Cambridge University Press)
- [3] Einstein A 1956 *Investigation on the Theory of Brownian Motion* (New York: Dover)
- [4] Rössler E 1990 *Phys. Rev. Lett.* **65** 1595
- [5] Ehlich D and Sillescu H 1990 *Macromolecules* **23** 1600
- [6] Fujara F, Geil B, Sillescu H and Fleischer G 1992 *Z. Phys. B* **88** 95
- [7] Hooker J C and Torkelson J M 1995 *Macromolecules* **28** 7683
- [8] Cicerone M T and Ediger M D 1996 *J. Chem. Phys.* **102** 471
- [9] Hall D B, Dhinojwala A and Torkelson J M 1997 *Phys. Rev. Lett.* **79** 103
- [10] Pollak G L and Eaycart J J 1985 *Phys. Rev. A* **31** 980
- [11] Berthier L 2004 *Phys. Rev. E* **69** 020201(R)
- [12] Liu C Z W and Oppenheim I 1996 *Phys. Rev. E* **53** 799
- [13] Sillescu H 1999 *J. Non-Cryst. Solids* **243** 81
- [14] Nicodemi M and Coniglio A 1998 *Phys. Rev. E* **56** R39
- [15] Angell C A, Richards B E and Velikov V 1999 *J. Phys.: Condens. Matter* **11** A75
- [16] Angelani L, Parisi G, Ruocco G and Viliiani G 1998 *Phys. Rev. Lett.* **81** 4648

- [17] Ye J, Hattori T, Nakatsuka H, Mazuyama Y and Ishikawa M 1997 *Phys. Rev. B* **56** 5286
- [18] Androzzì L, Di Schino A, Giordano M and Leporini D 1997 *Europhys. Lett.* **38** 669
- [19] Androzzì L, Donati C, Giordano M and Leporini D 1996 *Mater. Res. Soc. Proc.* **407** 233
- [20] Androzzì L, Giordano M and Leporini D 1998 *J. Non-Cryst. Solids* **235–237** 219
- [21] Faetti M, Giordano M, Leporini D and Pardi L 1999 *Macromolecules* **32** 1876
- [22] Heuberger G and Sillescu H 1996 *J. Phys. Chem.* **100** 15255
- [23] Cicerone M T, Blackburn F R and Ediger M D 1995 *J. Chem. Phys.* **102** 471
- [24] Cicerone M T and Ediger M D 1995 *J. Chem. Phys.* **104** 7210
- [25] Androzzì L, Cianflone F, Donati C and Leporini D 1996 *J. Phys.: Condens. Matter* **8** 3795
- [26] Androzzì L, Faetti M, Giordano M, Palazzuoli D and Galli G 2001 *Macromolecules* **34** 7325
- [27] Moro G and Freed J H 1980 *J. Phys. Chem.* **84** 2837
- [28] Moro G and Freed J H 1981 *J. Chem. Phys.* **74** 3757
- [29] Lee M H, Kim I M and Dekeyser R 1984 *Phys. Rev. Lett.* **52** 1579
- [30] Goldstein M 1969 *J. Chem. Phys.* **51** 3728
- [31] Androzzì L, Bagnoli M, Faetti M and Giordano M 2002 *J. Non-Cryst. Solids* **303** 262
- [32] Androzzì L, Di Schino A, Giordano M and Leporini D 1998 *Phil. Mag. B* **77** 547
- [33] Androzzì L, Faetti M, Giordano M, Zulli F and Castelvetro V 2004 *Phil. Mag. B* **84** 1555
- [34] Androzzì L, Bagnoli M, Faetti M and Giordano M 2002 *Phil. Mag. B* **82** 409
- [35] Muus L T and Atkins P W (ed) 1972 *Electron Spin Relaxation in Liquids* (New York: Plenum)
- [36] Androzzì L, Donati C, Giordano M and Leporini D 1992 *Phys. Rev. A* **46** 6222
- [37] Giordano M, Grigolini P, Leporini D and Marin P 1985 *Adv. Chem. Phys.* **62** 321
- [38] Rose M E 1957 *Elementary Theory of the Angular Momentum* (New York: Wiley)
- [39] Alessi L, Androzzì L, Faetti M and Leporini D 2001 *J. Chem. Phys.* **114** 3631
- [40] Keana J F 1978 *Chem. Rev.* **78** 37
- [41] Stickel F, Fischer E W and Richert R 1996 *J. Chem. Phys.* **104** 2043
- [42] Laughlin W T and Uhlmann D R 1972 *J. Phys. Chem.* **76** 2317
- [43] Cukiermann M, Lane J W and Uhlmann D R 1973 *J. Chem. Phys.* **59** 3639
- [44] Enright G D and Stoicheff B P 1976 *J. Chem. Phys.* **64** 3658
- [45] Li G, Du W M, Sakai A and Cummins H Z 1992 *Phys. Rev. A* **46** 3343
- [46] Yang Y and Nelson K A 1995 *Phys. Rev. Lett.* **74** 4883
- [47] Greet R J and Turnbull D J 1966 *J. Chem. Phys.* **46** 1243
- [48] Bartsch E, Fujara F, Legrand J F, Petry W, Sillescu H and Wuttke J 1995 *Phys. Rev. E* **52** 738
- [49] Steffen W, Patkowski A, Glaser H, Meier G and Fischer E W 1994 *Phys. Rev. E* **49** 2992
- [50] Gotze W 1999 *J. Phys.: Condens. Matter* **11** A1
- [51] Androzzì L, Giordano M and Leporini D 1992 *Appl. Magn. Reson.* **4** 279
- [52] Ye J Y, Hattori T, Nakatsuka H, Maruyama Y and Ishikawa M 1997 *Phys. Rev. B* **56** 5286
- Bartoš J, Sauša O, Krištiak J, Blochowicz T and Rössler E 2001 *J. Phys.: Condens. Matter* **13** 11473
- Bartoš J, Sauša O, Bandzuch P, Zrubcov J and Krištiak J 2002 *J. Non-Cryst. Solids* **307–310** 417
- Dlubek G, Sen Gupta A, Pionteck J, Krause-Rehberg R, Kaspar H and Lochhaas K H 2004 *Macromolecules* **37** 660
- [53] Sastry S, Debenedetti P G and Stillinger F H 1998 *Nature* **393** 554
- [54] Stillinger F H and Weber T A 1984 *Science* **225** 983
- [55] Kob W and Andersen H C 1995 *Phys. Rev. E* **51** 4626
- [56] Takahara S, Ishikawa M, Yamamuro O and Matsuo T 1999 *J. Phys. Chem. B* **103** 792
- [57] Ferrer M L, Lawrence C, Demirjian B G, Kivelson D, Alba-Simionesco C and Tarjus G 1998 *J. Chem. Phys.* **109** 8010
- [58] Schug K U, King H E Jr and Bomer R 1998 *J. Chem. Phys.* **109** 1472
- [59] Angell C A, Ngai K L, McKenna G B, McMillan P F and Martin S W 2000 *J. Appl. Phys.* **88** 3113